

Coupled-Resonator Optical Near-Field Lithography

Mankei Tsang^{1,*} and Demetri Psaltis^{1,2}

¹*Department of Electrical Engineering, California Institute of Technology, Pasadena, California 91125, USA*

²*Institute of Imaging and Applied Optics, Ecole Polytechnique Fédérale de Lausanne, CH-1015 Lausanne, Switzerland*

The problem of pattern formation in resonantly-enhanced near-field lithography by the use of dielectric or plasmonic planar resonators is investigated. Sub-diffraction-limited bright or dark spots can be produced by taking advantage of the rotational invariance of planar resonators. To increase the spatial bandwidth of the resonant enhancement, an array of coupled planar resonators can open up a band of Bloch resonances, analogous to coupled-resonator optical waveguides.

A major limitation of current near-field imaging systems is the extreme proximity between the detector and the object. In lithography, biological imaging, and optical data storage applications, any contact with the lithographic mask, biological sample, or optical data storage medium potentially causes damage and is undesirable in practice. The detector is usually required to be close because the subwavelength information of the object is carried by evanescent waves, which decay exponentially. To increase the working distance, evanescent waves can be amplified by passive optical resonators, such as dielectric slabs [1, 2], photonic crystals [3], plasmonic slabs [4, 5, 6], and negative-refractive-index slabs [4]. The magnitude of the amplification is proportional to Q , the quality factor of the resonance [2], making the use of low-loss dielectric structures most promising for near-field imaging applications in the near future. Since the spatial bandwidth of each resonance is inversely proportional to Q , however, a resonator can only amplify certain sinusoidal patterns. An ideal lossless negative-index slab would not suffer from this trade-off, but such a material is impossible to fabricate by current technology.

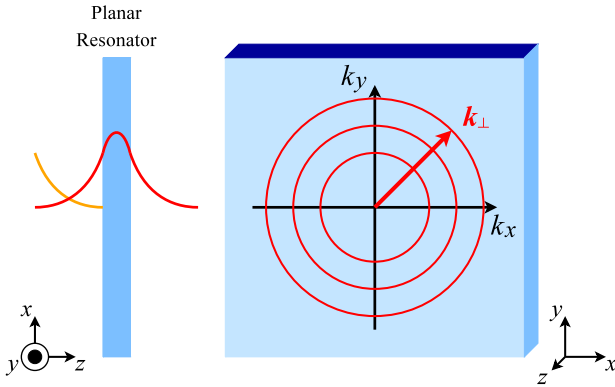


FIG. 1: Left: Evanescent wave coupled into a resonance mode can be enhanced on the other side of the resonator. Right: For an infinite planar resonator, the resonance modes lie on circles in the transverse spatial frequency domain due to rotational invariance.

Fortunately, complex patterns can still arise from the superposition of sinusoidal waves in an ordinary resonator, thanks to Fourier. Consider a planar resonator,

such as a dielectric or plasmonic slab, in the $x - y$ plane, as shown in Fig. 1. An evanescent wave decaying in z and impinging upon the resonator can be amplified, if its transverse wave vector, $\mathbf{k}_\perp \equiv k_x \hat{\mathbf{x}} + k_y \hat{\mathbf{y}}$, coincides with that of a resonance mode. Because an infinite planar resonator is rotationally invariant, the resonance condition depends on the magnitude of \mathbf{k}_\perp but not the direction of \mathbf{k}_\perp . Hence, a planar resonator always possesses a continuum of azimuthally degenerate modes. In practice, the finite size of the resonator means that the system is not strictly rotationally invariant, but the approximation is expected to be accurate for modes near the center of a large resonator.

Exciting all the azimuthally degenerate modes produces evanescent Bessel beams [7], which can be especially useful for lithography. The Bessel modes can be excited, for example, by placing a solid immersion lens [8] near the resonator [2]. For the transverse-electric (TE) resonance modes, the free-space electric field in cylindrical coordinates (ρ, ϕ, z) is in general given by

$$\mathbf{E}(\rho, \phi, z) = \int_{-\pi}^{\pi} d\theta [\hat{\rho} \sin(\phi - \theta) + \hat{\phi} \cos(\phi - \theta)] f(\theta) \exp[ik_\perp \rho \cos(\phi - \theta) - \kappa z], \quad (1)$$

where $f(\theta)$ is an arbitrary complex function, k_\perp is the magnitude of \mathbf{k}_\perp of a resonant mode, which must be larger than the free-space wavenumber $k_0 \equiv \omega/c$, and $\kappa \equiv (k_\perp^2 - k_0^2)^{1/2}$ is the decay constant. Apart from the exponential decay, the evanescent Bessel beam shapes remain invariant along z , so one can put the detector or the photoresist farther away from the resonator and still observe the same, albeit attenuated, profile. Setting $f(\theta) = 1$, for instance, gives a first-order Bessel beam,

$$\mathbf{E}(\rho, \phi, z) = i\hat{\phi} J_1(k_\perp \rho) \exp(-\kappa z), \quad (2)$$

which has a subwavelength dark spot in the middle. As the resonator is also translationally invariant in the $x - y$ plane, we can destructively interfere the first-order Bessel beam with one slightly displaced in x and obtain a “dipole” resonance mode,

$$\mathbf{E}(\rho, \phi, z) = i \frac{\partial}{\partial x} [\hat{\phi} J_1(k_\perp \rho)] \exp(-\kappa z), \quad (3)$$

which has two dark spots separated by a sub-diffraction-limited distance of $3.68/k_{\perp}$. The two examples of TE Bessel modes are plotted in Fig. 2. Other resonant patterns are clearly possible by specifying $f(\theta)$, or equivalently, superimposing displaced Bessel modes.

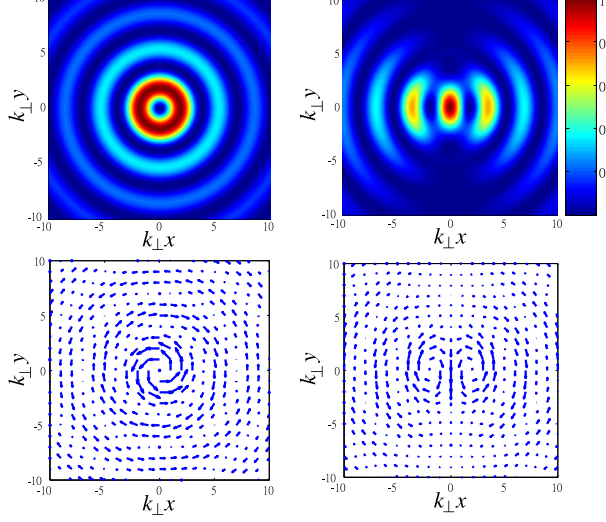


FIG. 2: Free-space electric energy (top row) and electric field (bottom row) plots of the TE first-order Bessel mode (left column) and the dipole mode (right column).

For the transverse-magnetic (TM) modes, on the other hand, the free-space electric field is

$$\begin{aligned} \mathbf{E}(\rho, \phi, z) \\ = \int_{-\pi}^{\pi} d\theta \left[\hat{\rho} \cos(\phi - \theta) - \hat{\phi} \sin(\phi - \theta) + \hat{z} \frac{ik_{\perp}}{\kappa} \right] \\ \times f(\theta) \exp [ik_{\perp}\rho \cos(\phi - \theta) - \kappa z]. \end{aligned} \quad (4)$$

For $f(\theta) = 1$,

$$\mathbf{E}(\rho, \phi, z) = i \left[\hat{\rho} J_1(k_{\perp}\rho) + \hat{z} \frac{k_{\perp}}{\kappa} J_0(k_{\perp}\rho) \right] \exp(-\kappa z). \quad (5)$$

The beam profile depends on k_{\perp} . In the diffraction limit, $k_{\perp} = k_0$, the $\hat{\rho}$ component vanishes, and the beam profile contains a diffraction-limited bright spot. In the super-resolution limit, $k_{\perp} \gg k_0$, the total electric-field energy is the incoherent superposition of the two polarizations, which has a smoother beam shape but a slightly wider peak than the zeroth-order Bessel function. A TM dipole mode can also be obtained by differentiating Eq. (5) with respect to x . The TM Bessel modes are plotted in Fig. 3.

Despite the presence of Bessel modes, near-field pattern formation with just one value of k_{\perp} is still fairly limited. In particular, the side rings of Bessel modes are undesirable for lithography. Here we show that an array of coupled planar resonators can provide a band of resonance modes that help solve this problem.

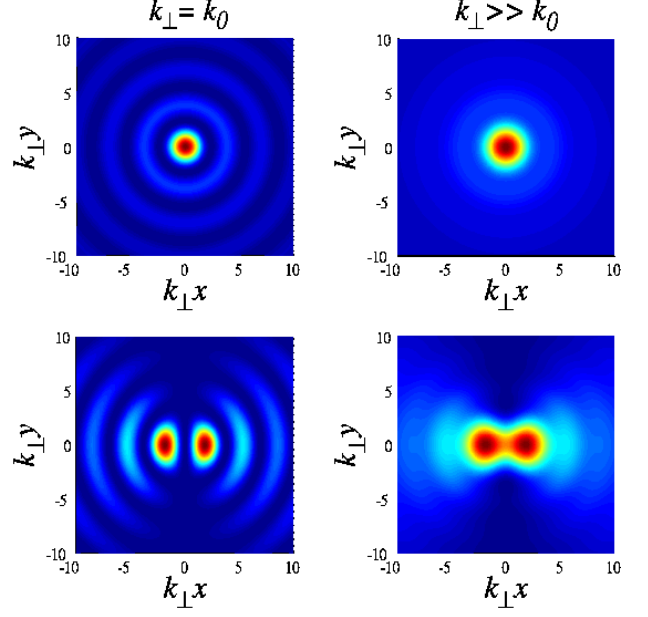


FIG. 3: Free-space electric energy plots of the TM zeroth-order Bessel mode (top row) and the dipole mode (bottom row) in the diffraction limit (left column) and in the super-resolution limit (right column).

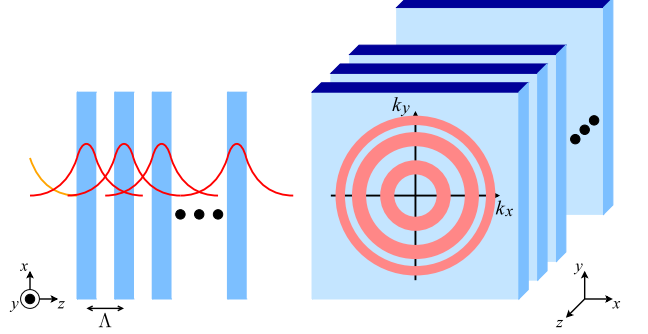


FIG. 4: Coupled planar resonators possess Bloch resonances that enable evanescent-wave amplification for continuous bands of spatial frequencies.

The physics of periodic layered media is well known [9, 10]. For simplicity, we study the problem in terms of light propagation along x in coupled waveguides, the supermodes of which are identical to the resonance modes in the evanescent coupling geometry in the limit of weak coupling and lossless media, since the approximations used are identical in both cases. Consider an array of N identical planar resonators with period Λ along z , as depicted in Fig. 4. To be specific, we shall consider the TE polarization only. Let the permittivity of one resonator be $\epsilon'(z)$, and the electric field be

$$E_y(x, z) = \sum_n A_n(x) \mathcal{E}_0(z - n\Lambda) \exp(ik_{\perp 0}x), \quad (6)$$

where $\mathcal{E}_0(z)$ is an unperturbed eigenmode electric field

of the resonator with $\epsilon'(z)$, normalized according to $[k_{\perp 0}/(2\omega\mu_0)] \int_{-\infty}^{\infty} dz[\mathcal{E}_0(z)]^2 = 1$, and $k_{\perp 0}$ is the spatial frequency along x of the unperturbed mode. Invoking the weak coupling approximation, we obtain [11]

$$\frac{dA_n}{dx} = i\beta A_n + i\gamma(A_{n-1} + A_{n+1}), \quad (7)$$

where $\beta \equiv (\omega/4) \int_{-\infty}^{\infty} dz[\epsilon(z) - \epsilon'(z)][\mathcal{E}_0(z)]^2$ and $\gamma \equiv (\omega/4) \int_{-\infty}^{\infty} dz[\epsilon(z) - \epsilon'(z)]\mathcal{E}_0(z)\mathcal{E}_0(z - \Lambda)$. The coupled-mode equations for the TM polarization are the same, with slightly different definitions of β and γ . The N coupled-mode equations (7) give rise to N supermodes. In the limit of infinite N , the supermodes become Bloch modes,

$$a_K \equiv \sum_n A_n \exp(-inK\Lambda), \quad (8)$$

$$a_K \propto \exp[i\beta x + 2i\gamma \cos(K\Lambda)x], \quad (9)$$

which exist in a continuous band of spatial frequencies, with a width controlled by the coupling constant γ ,

$$k_{\perp 0} + \beta - 2\gamma < k_{\perp} < k_{\perp 0} + \beta + 2\gamma. \quad (10)$$

The coupling constant can be manipulated by varying the distance between each pair of resonators or changing the permittivity of the gap material. In the evanescent coupling geometry, the Bloch modes enable evanescent-wave amplification for a band of spatial frequencies around the resonance of one planar resonator.

The physics of coupled planar resonators in the spatial domain is analogous to the coupled-resonator optical waveguide (CROW) in the time domain [12], in which an array of coupled high- Q resonators open up a band of resonant frequencies. Due to rotational invariance, the Bloch theory is valid regardless of the direction of \mathbf{k}_{\perp} , so the circles of resonances in the spatial frequency domain for one resonator become thick rings for coupled resonators, as depicted in Fig. 4. Furthermore, although our focus here is monochromatic light, coupled planar resonators are also a CROW in the time domain, and should therefore allow resonant transmission of three-dimensional spatiotemporal information.

The magnitude of evanescent-wave amplification by each supermode can be roughly estimated by comparing the energy of the supermode and the power dissipation, using the method described in [2]. Let Γ be the evanescent-wave reflection coefficient of the stack. When an incoming evanescent wave is resonantly coupled to the structure, the stored energy in each supermode is approximately proportional to $N \text{Im}\{\Gamma\}^2$, while the power dissipated at resonance is proportional to $\text{Im}\{\Gamma\}$. Using the definition of Q , the maximum magnitude of Γ , after appropriate units are introduced, is hence on the order of Q/N . The magnitude of the evanescent-wave transmission coefficient is approximately the same as $\text{Im}\{\Gamma\}$ at resonance.

The possibility of anomalous diffraction due to Bloch dispersion or a negative γ may also be useful for imaging. One way of investigating anomalous diffraction is to take the limit of infinitesimally thin layers and apply the effective medium theory [13, 14, 15, 16, 17, 18, 19], but the effective medium approximation is unable to account for resonant enhancement. A Bloch theory in more complex geometries, such as those studied in Refs. [15, 16, 17, 18, 19], will be of fundamental interest. Nonlinear propagation in periodic media is another interesting topic [20], although the problem has not been studied in detail in terms of the evanescent coupling geometry. The new physics that arises from nonlinear optics may lead to further improvement of resonantly enhanced near-field lithography.

Discussions with Zhiwen Liu, Andreas Vasdekis, James Adleman, and Konstantinos Makris are gratefully acknowledged. This work is supported by the National Science Foundation through the Center for the Science and Engineering of Materials (DMR-0520565) and the DARPA Center for Optofluidic Integration.

* Electronic address: mankei@optics.caltech.edu

- [1] M. Tsang and D. Psaltis, Opt. Lett. **31**, 2741 (2006).
- [2] M. Tsang and D. Psaltis, Opt. Express **15**, 11959 (2007).
- [3] C. Luo, S. G. Johnson, J. D. Joannopoulos, and J. B. Pendry, Phys. Rev. B **68**, 045115 (2003).
- [4] J. B. Pendry, Phys. Rev. Lett. **85**, 3966 (2000).
- [5] N. Fang, H. Lee, C. Sun, and X. Zhang, Science **308**, 534 (2005).
- [6] D. O. S. Melville and R. J. Blaikie, Opt. Express **13**, 2127 (2005).
- [7] S. Ruschin and A. Leizer, J. Opt. Soc. Am. A **15**, 1139 (1998).
- [8] S. M. Mansfield and G. S. Kino, Appl. Phys. Lett. **57**, 2615-2616 (1990).
- [9] P. Yeh, A. Yariv, C.-S. Hong, J. Opt. Soc. Am. **67**, 423 (1977).
- [10] P. Yeh, *Optical Waves in Layered Media* (Wiley, New York, 2005).
- [11] A. Yariv, *Quantum Electronics* (Wiley, New York, 2001).
- [12] A. Yariv, Y. Xu, R. K. Lee, and A. Scherer, Opt. Lett. **24**, 711 (1999).
- [13] S. M. Rytov, Sov. Phys. JETP **2**, 466 (1956).
- [14] S. A. Ramakrishna, J. B. Pendry, M. C. K. Wiltshire, and W. J. Stewart, J. Mod. Opt. **50**, 1419-1430 (2003).
- [15] A. Salandrino and N. Engheta, Phys. Rev. B **74**, 075103 (2006).
- [16] Z. Jacob, L. V. Alekseyev, and E. Narimanov, Opt. Express **14**, 8247 (2006).
- [17] Z. Liu, H. Lee, Y. Xiong, C. Sun, and X. Zhang, Science **315**, 1686 (2007).
- [18] I. I. Smolyaninov, Y.-J. Hung, and C. C. Davis, Science **315**, 1699 (2007).
- [19] M. Tsang and D. Psaltis, Phys. Rev. B , in press.
- [20] D. N. Christodoulides, F. Lederer, and Y. Silberberg, Nature (London) **424**, 817 (2003).